Quantum effects in the dynamics of deeply supercooled water

A. L. Agapov, A. I. Kolesnikov, V. N. Novikov, R. Richert, and A. P. Sokolov

Phys. Rev. E **91**, 022312 — Published 26 February 2015

DOI: 10.1103/PhysRevE.91.022312

Quantum Effects in the Dynamics of Deeply Supercooled Water

A. L. Agapov[1,2], A. I. Kolesnikov[3], V. N. Novikov[1,2], R. Richert[4], A. P. Sokolov[1,2]

[1] Department of Chemistry and Joint Institute for Neutron Sciences, University of Tennessee, Knoxville, TN 37996, USA

[2] Chemical Sciences Division, Oak Ridge National Laboratory, Oak Ridge, TN 37831, USA

[3] Chemical and Engineering Materials Division, Oak Ridge National Laboratory, Oak Ridge, TN 37831, USA

[4] Department of Chemistry and Biochemistry, Arizona State University, Tempe, Arizona 85287, USA

Abstract

Despite its simple chemical structure water remains one of the most puzzling liquids with many anomalies at low temperatures. Combining neutron scattering and dielectric relaxation spectroscopy we show that quantum fluctuations are not negligible in deeply supercooled water. Our dielectric measurements revealed the anomalously weak temperature dependence of structural relaxation in vapor deposited water close to the glass transition temperature T_g~136K. We demonstrate that this anomalous behavior can be explained well by quantum effects. These results have significant implications for our understanding of water dynamics.

I. Introduction

Water is the most important liquid for our life. Water molecule has relatively simple structure consisting of one oxygen and two hydrogen atoms. Yet, its behavior, especially at low temperatures, remains a great puzzle and is a subject of many debates [1-10]. Even the glass transition temperature T_g of bulk water remains a topic of discussions [1-6,11-15]. Dielectric spectroscopy measurements on confined water suggest that the relaxation time of the main dielectric relaxation process reaches $\tau_\alpha \sim 10^2$-10^3 s (usually accepted as T_g) at temperatures that depend strongly on confinement [11,16]. Recently the authors of [11] tried to estimate the bulk water T_g using water in various confinements. They suggested that T_g of bulk water can be as high as 210K [11], probably the highest T_g ever suggested for water. Most of the authors though agree that T_g of bulk low-density amorphous ice (LDA) and of vapor deposited amorphous solid water (ASW) is in the range $T_g \sim$125-136 K [4,13,15,17-24]. This T_g agrees well with the crystallization kinetic of LDA and ASW water [25], and it would be difficult to explain their crystallization around 135-140K if T_g is above 200K.

Another puzzling behavior of water appears as an apparent change in the temperature dependence of structural relaxation around 210-235K [2, 3, 26-28]. There are many papers suggesting existence of a liquid-liquid transition in water around this temperature range [2,6,9,29-38]. However, most of the experimental results are obtained on confined water and water mixtures [2,5,6,39-41], and it remains unclear how much these results can be extrapolated to a bulk water, and how much they can be affected by phase separation (e.g. the case of water-glycerol mixtures [29,42]). Even computer simulations have intense discussion about the existence of two phase of supercooled water [37,43]. Recent detailed analysis of simulations of ST2 water model [37] revealed a coexistence of two metastable liquid states with different

densities. However, it is not obvious how much the ST2 model reproduce the real bulk water. Experimental results on X-ray diffraction of supercooled water obtained by fast cooling of water droplets revealed no phase transition down to T ~227K [10]. Instead, the authors observed smooth variation in the diffraction peaks reflecting smooth improving of the tetrahedral structure upon cooling [8,10]. Moreover, extrapolation of their data to lower temperatures agrees well with the $S(Q)$ of LDA [10].

The estimated temperature dependence of viscosity $\eta(T)$ or the relaxation time $\tau_\alpha(T)$ in ASW at temperatures close to the expected T_g~136K [3, 25] is another puzzle. It behaves according to the Arrhenius law, $\tau_\alpha = \tau_0 \exp(E_a/k_B T)$, with rather low activation energy E_a. The temperature behavior of glass-forming liquids is usually characterized by the fragility index m defined as [44]:

$$m = \left. \frac{d \log_{10} \tau_\alpha}{d(T_g/T)} \right|_{T=T_g} \quad (1)$$

The fragility index quantifies the deviation of the temperature dependence of structural relaxation from a simple Arrhenius dependence. Materials that exhibit Arrhenius-like temperature dependence are called strong and those with pronounced non-Arrhenius variations of τ_α are called fragile. The latter might have a fragility index of m~100 and higher, while the least fragile materials such as SiO_2 and BeF_2 have m~20-22. According to earlier indirect estimates [25], the fragility of water at low temperatures might be m ~ 20, similar to the least fragile materials e.g. SiO_2. Such strong behavior is very unusual for a hydrogen bonding systems [45]. Moreover, this low-temperature behavior of water (T<150K) disagrees with the well-studied high temperature (T > 235K) regime that exhibits relaxation with a non-Arrhenius behavior that cannot be extrapolated to the low-temperature data [25]. These observations have

been used by many researchers to support the idea of the underlying liquid-liquid phase transition in water in the temperature range T ~210-235K [2, 5,29-41].

The major experimental problem in resolving these puzzles is the fast crystallization of bulk water in the temperature range 230K – 160K that prevents studies of equilibrium amorphous bulk water. Recently, on purely theoretical grounds, it was proposed [46] that structural relaxation close to T_g in liquids of light molecules, including water, may be significantly influenced by quantum effects, leading to abnormally low fragility. Additionally, various simulations of water demonstrated that even at ambient temperature, quantum effects lead to an increase of diffusion coefficients and a decrease of relaxation times by ~15-50% [47, 48]. Such quantum effects should be much more pronounced at lower temperatures, close to the T_g. Indeed, significant quantum effects in proton momentum distribution in supercooled water were found in simulations [49] and in a deep inelastic neutron scattering experiment [50]. These effects lead, in particular, to the excess mean kinetic energy of protons [50].

This paper focuses on the analysis of quantum effects in the structural relaxation of vapor deposited water around its glass transition temperature. We show that quantum fluctuations play an important role in the dynamics of deeply supercooled water. Analysis of neutron scattering and dielectric relaxation spectroscopy data reveals that quantum fluctuations are not negligible and can explain the unusual sub-Arrhenius behavior of dynamics in supercooled water at temperatures close to T_g ~136K.

II. Experimental Methods

A. Sample preparation

Water (Chromasolv Plus) was purchased from Sigma Aldrich. Prior to the deposition onto a surface of dielectric electrodes water was degassed via freeze-thaw cycling. Water was deposited

at a rate of about 5 nm/sec onto interdigitated electrodes (IDE) held at T =14K. These conditions result in formation of amorphous film [51, 52]. The thickness of the deposited film was about 20 μm. After the deposition the film was heated to 148.5K at a rate 0.4 K/min and annealed at this temperature for 10 min.

B. Dielectric spectroscopy measurements

Dielectric measurements of deposited water were carried out using the IDE cell [53] purchased from ABTECH Scientific, Inc (IME 1050.5-FD-Au-U). The IDE structure consists of 50 pairs of Au electrode fingers. Each finger has the dimensions of 4990 × 10 × 0.100 μm (l×w×h) with a spacing of 10 μm between electrodes. The geometric capacitance of IDE cell was calibrated at room temperature using air, isopropyl alcohol and water as reference materials. The IDE cell was placed onto a copper holder with silver paint applied between IDE and the holder to ensure good thermal contact. The holder was mounted onto the cold stage of a closed cycle He cryostat with high vacuum sample environment. Temperature was controlled with Lake Shore LS 340 controller using calibrated diode sensors. Temperature stability during the measurements was within ±0.01 K of the set point. Dielectric measurements were performed using a Solartron SI-1260 gain-phase analyzer in combination with a Mestec DM-1360 transimpedance amplifier. Measurements were performed in the frequency range of $2 \cdot 10^{-3}$ – 10^{7} Hz with the frequency density of 8 points/decade.

Initially, dielectric measurements were performed on the cooling cycle in the temperature range 148.5 – 136.5K with 2K intervals. To ensure that the film was stable over the course of dielectric experiment it was subsequently measured on the heating cycle in the same temperature range. Temperature ramping between set points on cooling and heating cycles was kept at a slow rate of

0.4 K/min in order to avoid crystallization. The dielectric spectra measured on cooling and subsequent heating agree well (Fig.1 a) indicating stability of the sample during the measurements. The onset of crystallization on the heating cycle was observed at temperatures 150 - 152K. Above that temperature the amplitude of the relaxation process was slowly, but irreversibly decreasing and the width of the spectrum was increasing (Fig.1 b). All the measurements, including samples preparation have been repeated several times, which verified the reproducibility of the results.

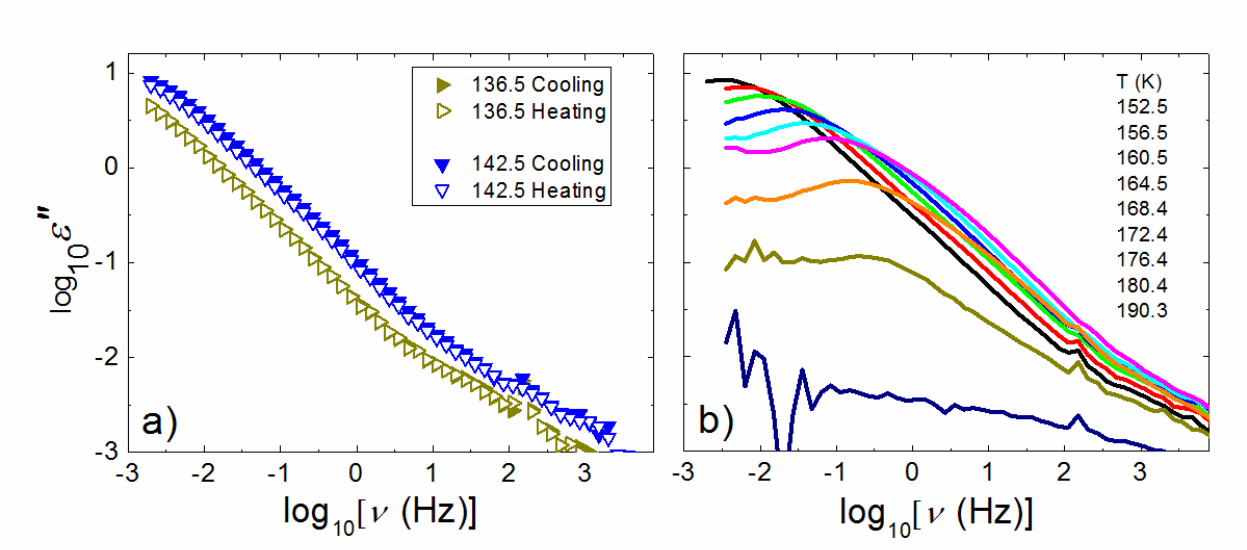

FIG. 1. (Color online) a) Dielectric loss spectra of amorphous water measured on initial cooling and subsequent heating cycles. Amorphous water is stable at temperature below 150K. b) Crystallization of deposited water film occurs at temperatures above 150K with main relaxation peak irreversibly decreasing in amplitude and broadening in width. The order of temperatures corresponds to the order of lines.

C. Analysis of the Dielectric Spectra

A detailed analysis shows that the loss spectrum can be fit by three relaxation processes (Figs. 2, 3), each one being well described by a symmetric Cole-Cole relaxation function, $\varepsilon'(\omega) + i\varepsilon''(\omega) = \Delta\varepsilon/[1+(i\omega\tau)^{\alpha}]$. The two largest in amplitude processes are almost Debye-like with the stretching parameter being $\alpha \sim 0.8$. The weakest visible dielectric process is strongly stretched, with Cole-Cole stretching parameter ~0.5 (Fig. 3). We emphasize that in order to obtain robust and consistent results, the fit functions were required to fit both dielectric loss and storage permittivity simultaneously (Fig. 2). Such restrictions help to avoid fit ambiguity and instability issues that are primarily responsible for the uncertainties in the relaxation time. The amplitude of the relaxation peak appears to be significantly lower than in bulk water at ambient temperature. This difference can be caused by experimental problems, e.g. not homogeneously deposited water, sample porosity. On the other hand, it can be also another anomalous behavior of water. For example, significant decrease of the amplitude of the dielectric relaxation peak with cooling at T <170K has been observed in earlier studies of LiCl-H_2O system [54].

The spectra at all temperatures form a consistent master plot (Fig. 3), with the exception of the spectrum at T =148.5K where the higher frequency component of the spectrum is more intense. We assign the main peak (the lowest frequency peak, Fig. 3) to the structural relaxation of the annealed ASW (LDA-like water) and refer to it as the α-process. It should be noted that bulk water as well as monohydroxy alcohols are known to have dielectrically active Debye-like processes with their origin still being a matter of debate [55-57]. But this discussion is beyond the scope of the current manuscript. The second peak (intermediate frequency, Fig. 3) presents ~1% of the total spectrum and might be assigned either to small amount of an HDA, or to some unrelaxed amorphous water that can be present in films deposited at low temperatures [58], or to a reorientation of a single hydrogen-bonded water molecule [56]. This peak is present in all the

spectra acquired in the range 148.5 – 136.5K and we refer to it as a β-process. At still higher frequencies (around 10^2 – 10^4 Hz) another weak process with contribution less than 0.1% of the total spectrum can be observed. We tentatively ascribed it to either dangling of OH- bonds or defect migration, and call it as a γ-process (Fig.3). We emphasize that the microscopic nature of the beta and gamma processes are not important for the main topic of this paper.

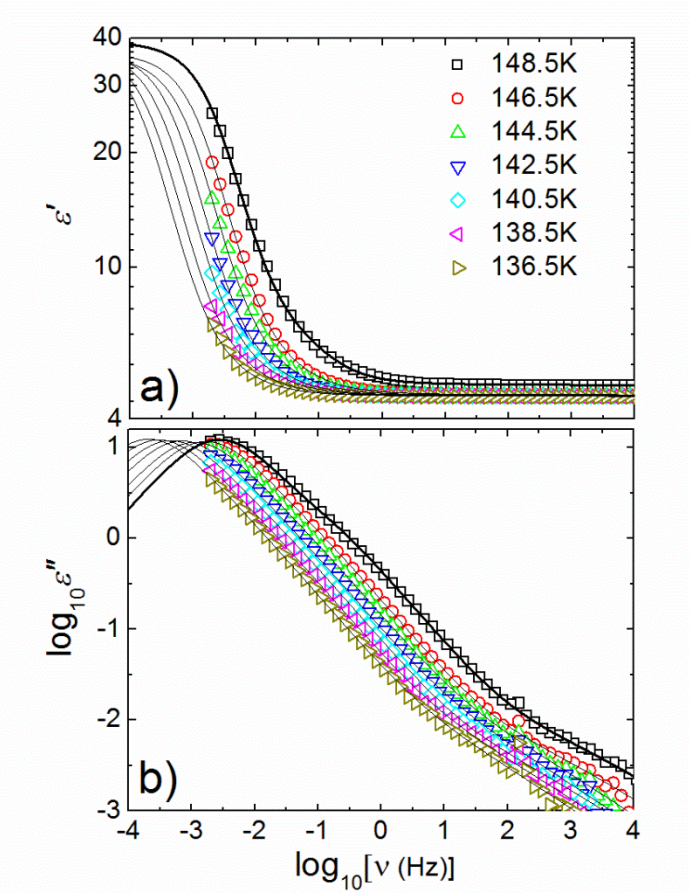

FIG. 2. (Color online) Dielectric spectra of amorphous water (symbols) measured on initial cooling cycle in terms of a) storage and b) loss permittivity. Solid lines present the simultaneous fit of the real and imaginary spectra by the sum of three Cole-Cole functions.

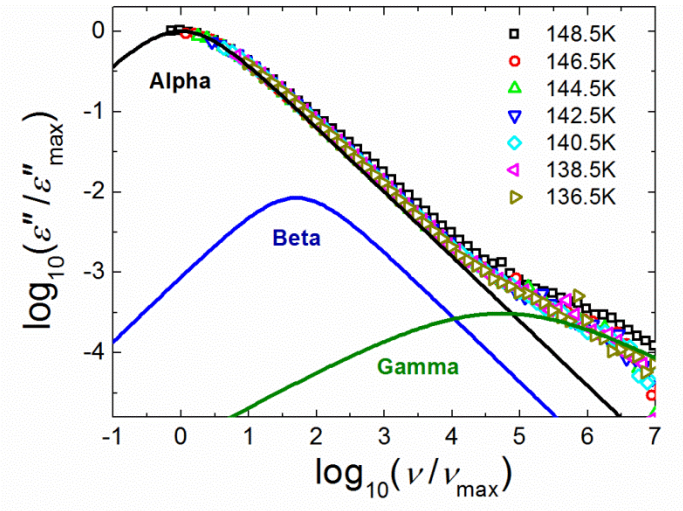

FIG. 3**.** (Color online) Time-temperature superposition plot of the dielectric loss. Here, solid lines represent contributions of the individual processes: black (upper curve) – α-relaxation, blue (middle curve) – β-relaxation, green (bottom curve) – γ-relaxation processes.

We note that there is some uncertainty associated with the relaxation time extracted from the dielectric spectra (Figs.1-3). However, this uncertainty is relatively small (due to high accuracy of the dielectric measurements). The maximum of the alpha relaxation process clearly appears in the measured frequency window at T =148.5K (Fig. 2b), allowing us to determine the relaxation time at this temperature without ambiguity. This relaxation peak is resolved even better at temperatures above 150K (Fig. 1b). However, we refrain from including these high temperature data because they are affected by crystallization. To extract the relaxation time at temperatures below 148K we have to make certain assumptions. First, the stretching parameters for all three relaxation processes were kept constant for all temperatures analyzed (0.8 for alpha and beta processes and 0.5 for gamma process). In addition, we have imposed a restriction that the dielectric strength of the alpha process cannot change significantly with temperature, only within the range less than 10%. The 10% change in dielectric strength restriction corresponds to effect

of temperature change from 136.5K to 148.5K on the $\Delta\varepsilon$ with the assumption that the Kirkwood-Fröhlich correlation factor remains constant for the sample in the given temperature range. Fitting procedure with such restrictions provided a robust fit for both ε' and ε" with the mean square deviation not greater than 0.05 for every spectrum (Fig. 2). The error in the relaxation time for the alpha process extracted using the above-described fitting procedure was less than 10% of the value. We have also tried fitting procedure using only two relaxation processes, those identified as alpha and gamma processes in Fig. 3. Such fitting required a use of stronger stretching for the alpha process, was giving a less robust fit with larger mean square deviation and larger error in the alpha relaxation time. However, the relaxation time itself remained unchanged, as it does not depend on stretching parameter for a Cole-Cole process.

D. Estimates of generalized density of vibrational states $g(E)$ from neutron scattering measurements.

The generalized density of vibrational states, $g(E)$, was directly obtained from the inelastic neutron scattering (INS) spectra. The INS spectra of deposited water and of low-density amorphous (LDA) water were taken from previous studies [59-61]. Briefly, the LDA sample was prepared from high density amorphous (HDA) ice by heating it to 117 K. The initial HDA-ice was produced by pressurizing ice-Ih at 77 K to about 10.5 kbar, and releasing the pressure to ambient at the same T. The deposited film was produced by water vapor condensation on the surface of an aluminum sample-can (hollow cylinder, 60 mm long and 10 mm inner diameter), which was kept below 15 K. The deposition processes were carried out for 45 h with a flow rate of 7 mg/h. The estimated sample thickness was 0.15 mm, which corresponds to the rate of sample growth of 3 μm/h. The deposited film was not annealed. The INS measurements were

done at T =5 K for the deposited sample and at 15 K for LDA sample using the time-of-flight spectrometer TFXA [62] at ISIS Spallation Neutron Source, UK. TFXA is the inverse-geometry spectrometer with all energies ("white") incident neutrons and fixed energy for registered neutrons ($E_R \approx 4$ meV) and has very good energy resolution $\Delta E/E \approx 2\%$ over a wide range of energy transfers, 2-500 meV. The spectra of the empty containers at the same temperatures were also measured and subtracted from the samples' data.

The measured INS spectra were transformed by standard programs to the dynamical structure factor, $S(Q,E)$, where Q and E are neutron momentum and energy transfer. In general, $S(Q,E)$ for hydrogen containing materials can be described by the equation (2), that includes scattering with absorption l and creation (k-l) of vibrational modes, single- and multi- phonon contributions:

$$S(Q,E) = \sum_{l,k} S_{l,k-l}(Q,E) = e^{-<u_H^2>Q^2} \sum_{l,k} \left(\frac{\hbar^2 Q^2}{6m_H}\right)^k \int dE_1 \dots dE_k \frac{g(E_1)\dots g(E_k)}{E_1 \dots E_k (k-l)!\, l!} \prod_{i=l+1}^{k} [n(E_i,T)+1] \prod_{j=1}^{l} n(E_i,T)\, \delta\left(E - \sum_{i=l+1}^{k} E_i + \sum_{j=1}^{l} E_j\right) \quad (2)$$

$$g(E) = \sum_j \left|\mathbf{e}_H(j,E_j)\right|^2 \delta(E - E_j) \quad (3)$$

$$< u_H^2 >= \frac{\hbar^2}{3m_H} \int \frac{g(E)}{E} \left[n(E,T) + \frac{1}{2}\right] dE \quad (4)$$

where m_H is mass of hydrogen atom, $n(E_j,T)=[\exp(E_j/k_BT)-1]^{-1}$ is the Bose population factor, and the summation in Eq. (3) goes over all normal vibrational modes.

The Eq. (2) was used to extract the one-phonon neutron scattering contribution by using the measured spectra and an iterative technique [58,60,63]. At the first step $g(E)$ was calculated using Eq. (2) and assuming that the measured data in the range up to 125 meV present the one-phonon spectrum. This spectrum was then used then to calculate the two-, three- and four-phonon neutron scattering contribution using Eqs. (2-4). At the second and subsequent steps, the difference between the experimental spectrum and the calculated multiphonon contribution was accepted as the new one-phonon spectrum. For the analyzed spectra the convergence was

reached in 3 iterations. Figure 4 shows the experimental $S(Q,E)$ spectrum and calculated one-phonon and multiphonon contributions for the LDA sample. We can see that the multiphonon contribution is small at low energies (E <70 meV) and increases significantly at higher energies. Thus the multiphonon correction of neutron scattering is important. The spectrum for the deposited sample were treated in a similar way and then was transferred to $g(E)$ spectrum.

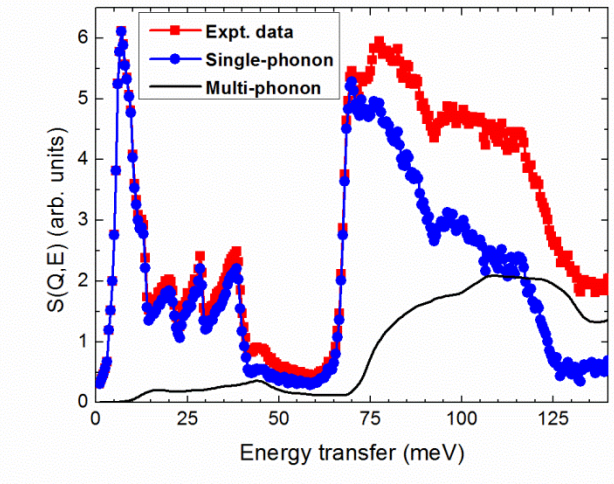

FIG. 4. (Color online) Dynamical structure factor $S(Q,E)$ for LDA sample obtained from the INS spectra measured at T =15K: The experimental spectrum (red curve with squares), calculated multiphonon (black line) and single-phonon (blue curve with circles) contributions.

III. Relaxation Time in Vapor Deposited Water

The relaxation times for all the processes extracted from the fits of the dielectric spectra are presented in Fig. 5. The alpha process τ_α reaches 1000s at T = 135.6K, which is close to the expected T_g of water. Thus, this relaxation process should be the signature of structural relaxation. It agrees with the estimates of viscosity controlling crystallization of water at these low temperatures [64] and with some earlier estimates of structural relaxation time in different types of amorphous water using dielectric spectroscopy [15,65,66] and differential scanning

calorimetry [67]. This result justifies our assignment of the α-process to the structural relaxation in amorphous water. In addition, Figure 5a presents the literature data on relaxation rate in cubic ice I_c [68, 69] and in hexagonal ice I_{hex} [70]. The activation energy for dielectric relaxation in cubic and hexagonal ices in the temperature range of interest is similar and amount to 44 and 47 kJ/mole, respectively. The activation energy for the alpha process (Fig. 5b) in amorphous water is much lower, only 36±1 kJ/mole. This suggests that the relaxation in the deposited amorphous water potentially has a different friction mechanism, with significantly lower energy barrier than in hexagonal or cubic ice in the same temperature range. However, we emphasize that the weakest in amplitude gamma process (Fig. 3) shows activation energy of 48 kJ/mole, similar to the values observed in crystalline ices.

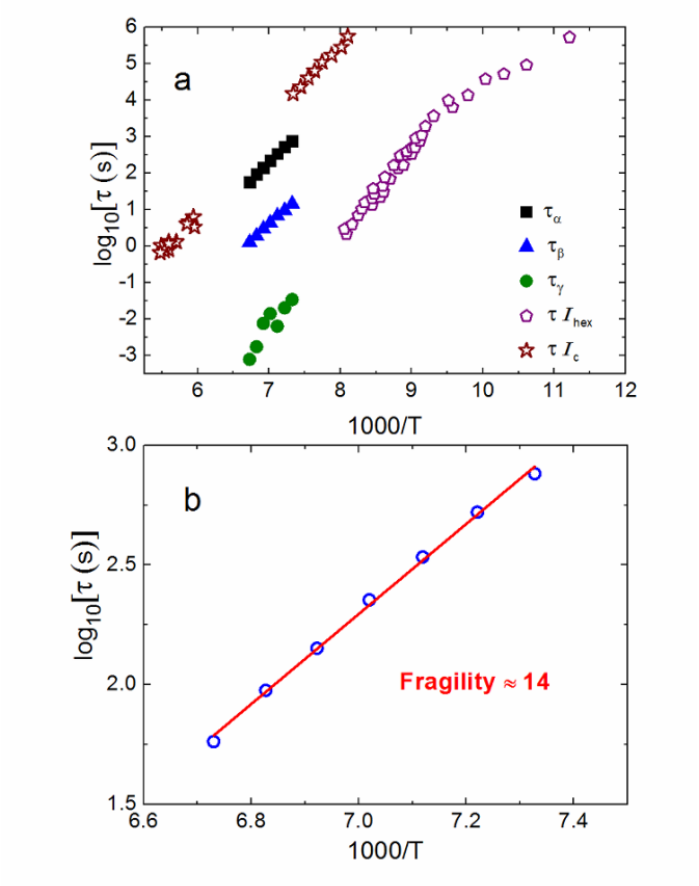

FIG. 5. (Color online) (a) Temperature dependence of characteristic relaxation times of different processes observed in the spectra of amorphous vapor-deposited water. In addition, empty stars are the data for cubic ice (from refs. [68, 69]) and empty pentagons present relaxation data of hexagonal ice (from ref. [70] and refs. therein). (b) Temperature dependence of τ_α vs inverse temperature (symbols) and its fit by the Arrhenius behavior (line). The latter provides estimates of the activation energy $E_a \approx 36\pm1$ kJ/mol and $\log_{10}[\tau_0\,(s)] = -10.9\pm0.3$.

Interestingly, the alpha relaxation time shows extremely slow temperature variation that leads to an unusual value of fragility $m \sim 14$, a low activation energy $E_a \approx 36\pm1$ kJ/mol, and an unphysically slow τ_0, $\log_{10}[\tau_0\,(s)] = -10.9\pm0.3$ (Fig.5b). These results are consistent with very recent dielectric studies by Böhmer and coworkers who also discovered that fragility of LDA water (prepared by annealing high-density amorphous (HDA) ice obtained by pressurizing ice-I_h at low-temperature) is $m \sim 14$ [71]. Our data together with the data by Böhmer and coworkers [71] might finally settle the discussion about T_g and fragility of deeply supercooled water. We want to emphasize that this value of the fragility is by far the lowest among known liquids. In that respect, deeply supercooled water indeed shows a "super-strong" behavior. It is even stronger than the least fragile liquids, such as SiO_2 and BeF_2. This result is very surprising because hydrogen bonding liquids usually have fragility indices in the range $m \sim 45$-90 [44, 45]. Moreover, this value of m is less than the minimum possible for a classical glass-forming system, $m \sim 17$. The latter corresponds to a purely Arrhenius relaxation from high temperatures with $\tau \sim \tau_0 \sim 10^{-14}$ sec to the glass transition with $\tau(T_g) \sim 10^3$ sec, or changing of viscosity from about $\eta \sim 10^{-4}$ Poise to $\eta \sim 10^{13}$ Poise. Extremely slow $\tau_0 \sim 10^{-11}$ s revealed in our case has never been

observed in any glass forming liquids, and presents a challenge to explain it using classical over-barrier relaxation mechanism.

IV. Nature of "Super Strong" Temperature Dependence of Dynamics in Water

Can this unusual temperature dependence of structural dynamics in amorphous water be caused by quantum effects, as it was proposed earlier in Ref. [46]? In order to answer this question, we analyze the ratio of zero point mean-square displacements (MSD) $\langle u_0^2 \rangle$ to the total MSD $\langle u^2(T) \rangle$ for hydrogen atoms. Vibrational MSD has been calculated from the generalized density of vibrational states, $g(E)$, for inter-molecular translational (0-40 meV) and librational (50-125 meV) bands in low-density amorphous (LDA) water and in low temperatures vapor-deposited water (see section II.D). The observed lower energy for the librational cutoff for the deposited sample (64 meV) compared to that for LDA sample (67.7 meV) means weaker hydrogen bonds (inset Fig.6). There is also an increase in the intensity (softening) of the low-energy part below 6 meV and significant shift (~ 4 meV) of all librational band to the low energies in the $g(E)$ spectrum for deposited sample in comparison to the LDA sample. All these suggest that the hydrogen atoms in the deposited sample appears to be more mobile than in LDA ice (Fig. 6). Using this $g(E)$, we calculate the temperature dependence of the total MSD in the harmonic approximation (assuming no significant change of $g(E)$ with T):

$$\left\langle u^2 \right\rangle \propto \int \frac{g(E)}{E}\left[n(E,T) + \frac{1}{2} \right] dE \qquad (5)$$

We neglect intra-molecular contribution to MSD in these calculations, because we assume that they are not important for the structural relaxation of water. The results (Fig. 6) show clearly that MSD at the expected T_g of water is dominated by the zero-point vibrations. Their contribution is ~55% of the total MSD in deposited water and ~61% in LDA.

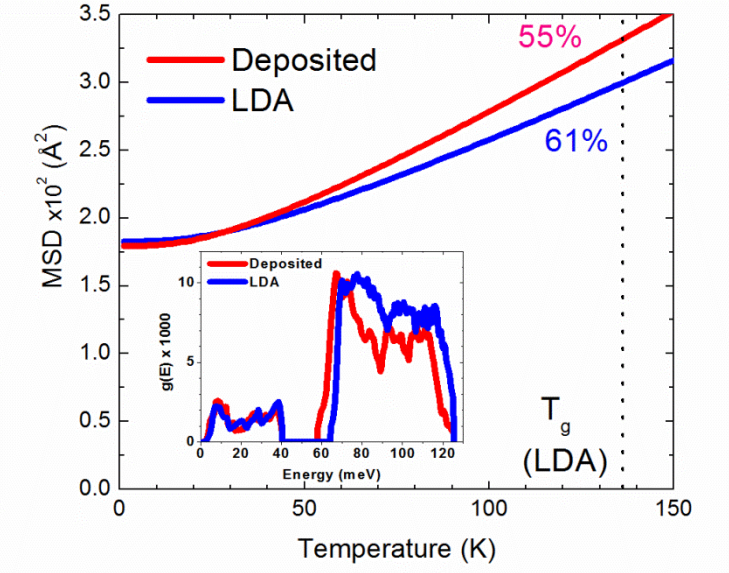

FIG. 6. (Color online) MSD in LDA water and in vapor-deposited at low temperatures water (solid lines). The dashed line marks the expected T_g ~136K of water. Zero-point vibrations dominate MSD and contribute 55% -61% to the total MSD of amorphous water at T_g. The inset shows the generalized vibrational density of states $g(E)$ for inter-molecular vibrations in LDA and deposited water obtained from INS spectra [59-61].

This strong contribution of quantum fluctuations should affect the structural relaxation of water. It was suggested in Ref. [46] that the effect of quantum fluctuations on $\tau_\alpha(T)$ can be taken into account by including zero-point MSD in the universal expression proposed in Ref. [72]:

$$\log_{10}\tau_\alpha = a_0 + a_1 <u^2(T_g)>/<u^2(T)> + a_2(<u^2(T_g)>/<u^2(T)>)^2 \qquad (6)$$

where a_0 = -10.922 (assuming $\tau_\alpha(T_g) = 10^3$ s), a_1 =1.622 and a_2 =12.3 are universal constants. This expression was derived in Ref. [72] by generalizing the well-known relationship $\tau_\alpha(T) = \tau_0 \exp(A/<u^2(T)>)$ suggested earlier [73-75], with the third term accounting for the local

fluctuations of the parameter A. It has been shown in Ref. [72] that the relationship (Eq. 6) holds well for many different glass-forming liquids. In Eq. (6), significant contribution of zero-point vibrations to the MSD should lead to very weak temperature variations of $\tau_\alpha(T)$ [46] and, respectively, to very low fragility of the system.

In order to answer the question whether unusual behavior can be caused by quantum effects, we use the Eq.(6) to estimate the expected temperature dependence of $\tau_\alpha(T)$. The total MSD of the deposited sample substituted in Eq.(6) predicts a slightly steeper variation of $\tau_\alpha(T)$ (Fig.7). However, $g(E)$ for the deposited water was measured on an un-annealed sample as described above. It is known that a deposition of water vapor below 30K results in formation of unrelaxed amorphous water [76]. After annealing at higher temperatures, the structure of deposited sample changes and becomes indistinguishable from an LDA-like phase [1, 77]. Thus, our dielectric data should be compared to the LDA neutron scattering data. Indeed, the total MSD of LDA water reproduces the experimental $\tau_\alpha(T)$ behavior surprisingly well (Fig.7). It is especially surprising taking into account our rough approximation that assumes harmonic behavior and neglects intra-molecular contributions to MSD, and it is possible that so good agreement is rather coincidental. If one subtracts zero point contribution from the total experimental MSD, a much steeper temperature dependence of $\tau_\alpha(T)$ is expected. It would correspond to a fragility of m ~35 and strongly disagrees with the experimental $\tau_\alpha(T)$ (Fig.7).

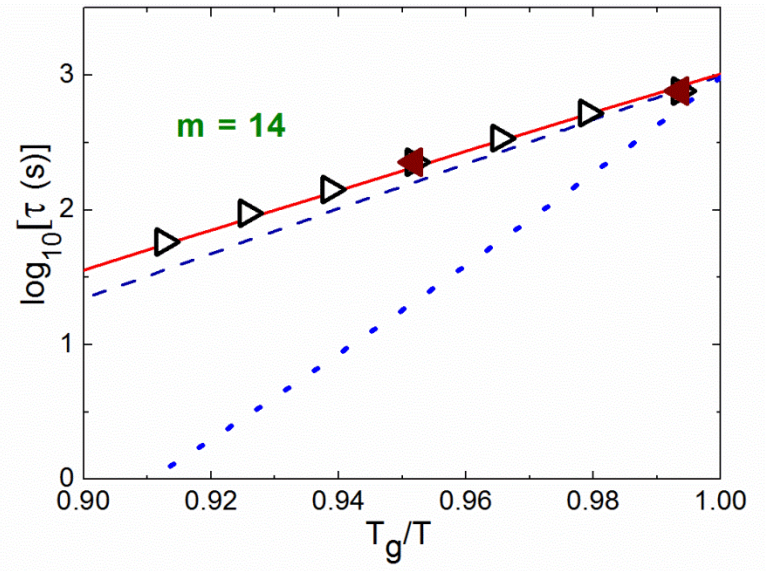

FIG. 7. (Color online) Temperature dependence of the isothermal dielectric relaxation time (symbols) in the vapor-deposited film of water measured on cooling (open symbols) and on heating (closed symbols) vs T_g/T. T_g=135.6K was chosen as the temperature at which τ_α =1000 s. The slope of the temperature dependence indicates an unusually low value of fragility, m=14. The lines show the expected temperature dependence of $\tau_\alpha(T)$ estimated using Eq.(6) with the total MSD of deposited un-annealed sample (dashed line), with the total MSD of LDA water (solid line) and MSD with excluded zero-point vibrations for LDA water (dotted line). The total MSD of LDA reproduces the temperature dependence of $\tau_\alpha(T)$ well and emphasizes the importance of quantum fluctuations in the dynamics of deeply supercooled water.

Let us now estimate the importance of anharmonic corrections for our analysis of fragility based on MSD. According to Ref. [78], anharmonic contributions in LDA ice are only ~6% at 123K, and might reach 7% at 140K (assuming linear extrapolation of the experimental data for the specific heat to 140K). Then the anharmonic contribution to the estimate of fragility (using Eqs. (1) and (6)) is of the order of $2\Delta u^2(T_g)/u^2(T_g) < 0.15$, where $\Delta u^2(T_g)$ is the anharmonic contribution to MSD. So, the anharmonic contribution to MSD indeed can be neglected in our analysis, because the difference of fragility with and without account for zero-point vibrations is about 250%, far larger than possible anharmonic corrections.

The presented analysis clearly demonstrates that quantum fluctuations in water are not negligible at temperatures close to the expected T_g. Their dominating role explains the unusual dynamic

behavior of structural relaxation in water without a need to invoke complex transformations between different types of water phases, a popular approach based on thermodynamic principles [1, 2, 5, 79]. The anomalously low value of fragility obtained for deposited water (Fig.7) and for LDA [71] might be the result of structural relaxation assisted by quantum fluctuations. With increasing temperatures, the role of these quantum effects will fade. As a result, $\tau_\alpha(T)$ will be controlled by usual thermally activated barrier-crossing type relaxation and return to a behavior typical for many liquids.

Thus, the quantum effects might also be at the origin of the so-called fragile-to-strong crossover in the dynamics of water. We want to stress at this point that the term fragile-to-strong crossover is actually misleading. By definition (eq.1), fragility is the measure of the steepness of the temperature dependence of τ_α at T_g. So, its estimates at significantly higher temperatures (e.g. from non-Arrhenius behavior) are not accurate and can be misleading. Nevertheless, the existence of the crossover is obvious from Fig. 8 where the higher temperature data for the structural relaxation time [80] are shown in addition to our low-T data. For comparison, $\tau_\alpha(T)$ for glycerol [81] is also shown. Relative to water, glycerol exhibits a smooth behavior with increase in apparent activation energy upon cooling and significantly higher fragility close to T_g. In contrast, water data suggests that the apparent activation energy drops at lower temperatures (Fig.8). The difference is that glycerol is much heavier molecule and quantum effects should be negligible around its T_g. Water is much lighter molecule than glycerol. As a result, quantum effects become not negligible and provide additional channel for structural relaxation in water at lower T.

Approximation of the high temperature data of bulk water using the Vogel-Fulcher-Tammann function $\tau = \tau_0 \exp[B/(T-T_0)]$ (Fig.8), indicates two interesting points: (i) τ_0 has reasonable value

~10^{-13}s, which is ~100 times faster than τ_0 of the low temperature behavior. This observation again emphasizes the anomalous low temperature dynamics of water that cannot be explained in classical picture of glass-forming liquids. (ii) Extrapolation to τ~10^3 s provides estimate of T_g ~198K (Fig.8) that gives T_g/T_m ratio ~0.7, close to the traditional 2/3 ratio (here T_m is the melting temperature). We speculate that this would be the relaxation behavior in bulk water in absence of quantum effects. However, at low T quantum fluctuations take over the relaxation process, lead to much slower temperature variation of structural relaxation and viscosity and shift the glass transition temperature to much lower value, $T_g \sim 0.5T_m$. This idea is consistent with the recent X-ray scattering studies of supercooled water that did not find any signs of the phase transitions down to T~227 K [10].

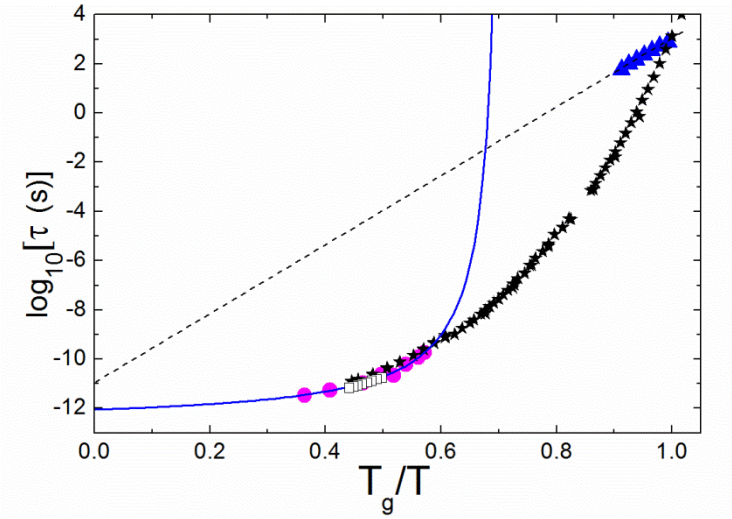

FIG. 8. (Color online) Comparison of low- and high temperature data for the structural relaxation time in water and in glycerol. Open squares – dielectric spectroscopy data in water [80], solid circles – shifted viscosity data [25], stars – dielectric spectroscopy data in glycerol [81]. The dashed line presents approximation of the low temperature behavior by an Arrhenius dependence, the solid line is approximation of the high temperature behavior using the Vogel-Fulcher-Tammann function.

V. Qualitative Estimates of Possible Tunneling

The importance of the quantum effects in the glass transition of water can be verified by estimates of the tunneling probability for the structural relaxation. Let us consider a simple model of tunneling from a potential well (Fig.9). A particle can escape a potential well either by a thermally activated jump or by tunneling through the barrier. In this simple model we use a harmonic potential till the top with the height E_b at the top (Fig. 9). The tunneling can go from each of the quantum levels with the energy E_n inside the well, so the total rate $\Gamma(T)$ for the particle to escape the well can be written as a sum of the thermal activation and tunneling contributions:

$$\Gamma(T) = \tau_0^{-1} \exp\left(-\frac{E_b - E_0}{T}\right) + \sum_n \Gamma(E_n, T)\, P(E_n, T). \qquad (7)$$

The first term in the right hand side of this expression corresponds to the over barrier thermal activation with the barrier height E_b (with subtracted zero-point energy E_0). The second term describes the tunneling from the quantum levels with energies $E_n < E_b$. In Eq. (7), $P(E_n,T) = \exp[-(E_n-E_0)/T]$ is the occupation of the level with the energy E_n (assuming $\exp(E_b/T) \gg \exp(E_0/T) \gg 1$ which is hold in our case), and $\Gamma(E_n,T)$ is the tunneling rate,

$$\Gamma(E_n, T) = \tau_0^{-1} \exp\left[-\frac{2}{\hbar}\int_{x_{1n}}^{x_{2n}} \sqrt{2M(U(x) - E_n)}\,dx\right] \qquad (8)$$

There are 3 parameters defining the potential $U(x)$ (Fig. 9): (i) the curvature at the bottom of the well, (ii) the barrier height E_b, and (iii) the barrier width at the bottom a (Fig. 9). Assuming that the rate (7) corresponds to the structural relaxation process, we can estimate the relaxation rate at different temperatures and fragility. The latter should be equal to $m \sim \log_{10}(\tau_\alpha(T_g)/\tau_0) \sim 17$ with $\tau_0 = 10^{-14}$ s for thermally activated process with a constant activation energy $E_b - E_0$. Increase of the

tunneling term should lead to decrease in fragility because it has weaker temperature dependence (lower apparent activation energy).

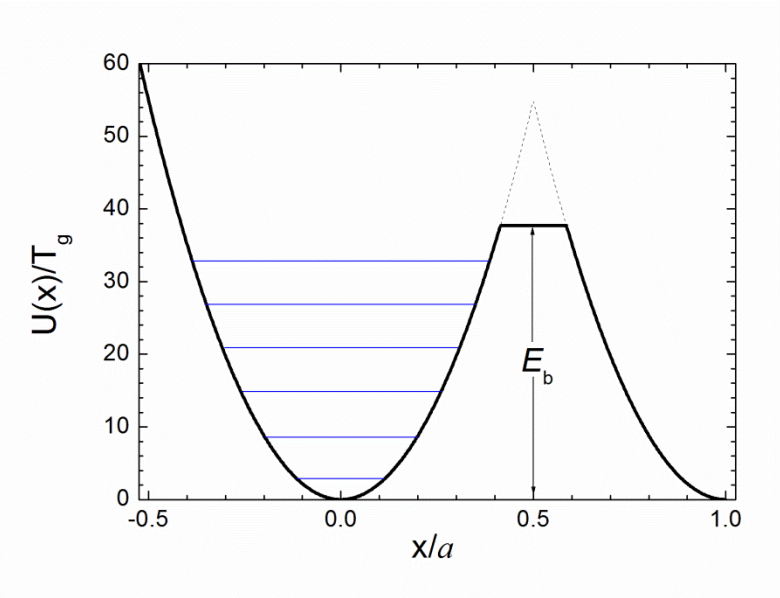

FIG. 9. (Color online) Schematic presentation of the potential well used to estimate tunneling probability. Lines in the well correspond to different quantum levels.

Dielectric spectroscopy measures reorientation of dipole moments that can be connected to rotation of H-atom(s) about the oxygen atom in water. In that case we can take the mass M in the Eq. (8) as a proton mass. Moreover, we can take the vibrational frequency in the well to be the librational mode. According to the vibrational spectrum of water (Fig.4) the librational mode is dominated by the peak in the range $\hbar\omega$ = 70-90 meV. This energy fixes the value of $\tau_0 \sim 10^{-14}$ s, and the curvature of the harmonic potential $U(x)$.

Using Eqs. (7),(8) we can estimate the potential parameters (barrier height E_b and the distance a) that would satisfy two requirements: (i) $\tau(T_g=136\text{K}) = 10^3$ s and (ii) fragility m = 14. We obtained $E_b - E_0$ = 46±1 kJ/mol rather independent of choice of librational $\hbar\omega$. This energy,

however, affect strongly the distance of the tunneling: We obtained $a = 2.2\pm0.02$ Å for $\hbar\omega = 90$ meV, and $a = 1.9\pm0.02$ Å for $\hbar\omega = 120$ meV. Taking into account the simplicity of the model, these values of a are in a reasonable agreement with the jump length 1.5-1.9 Å found in supercooled water by the quasielastic neutron scattering [82] and NMR [83]. The estimated activation energy ~ 46 kJ/mol is comparable to that found by dielectric spectroscopy in different ices, 44-57 kJ/mol [68-70, 84-87]. In spite of the very simplistic and schematic character of our estimate, it shows that the rotational tunneling effects can indeed lead to the experimentally measured value of fragility, $m = 14$, with the values of the model parameters corresponding to that of supercooled water. More accurate estimates are required to verify the probability of tunneling in realistic water potentials at low temperatures.

At that point we also want to mention the dielectric studies of confined water and some aqueous solutions [2,6,12,14,54]. These studies estimated the characteristic activation energy ~45-60 kJ/mol with reasonable $\tau_0 \sim 10^{-14}$-10^{-19} s. The latter is normal for relaxation in glass-forming liquids and is much shorter than the observed in our experiment $\tau_0 \sim 10^{-11}$ s. This relaxation in confined water and in aqueous solutions of sugars, polymers and proteins is often interpreted as ν- or ω- relaxation and is considered as a kind of secondary relaxation [12,14,54]. Based on its activation energy and τ_0, we suggest that this process is different from the one reported here for ASW and from the process reported in Ref. [71] for LDA.

We also want to emphasize that the suggestion of possible tunneling effects in crystalline ices has been discussed in several earlier papers [87- 89]. Many authors observed sub-Arrhenius temperature dependence of relaxation time (decrease in apparent activation energy with decrease in T, see e.g. Fig.5) and strong isotope effects in dielectric studies of ices [70,87], both are usual signs of the tunneling effects. Moreover, analysis of the relaxation in ice V revealed very low

energy barrier E ~23 kJ/mol at T <190K [84]. Analyzing these data we estimate $\tau_0 \sim 10^{-9}$ s for this relaxation in ice V, again being extremely slow relative to the usually expected value. The provided crude estimates and analysis of literature data on crystalline ices, all support the idea about significant probability of tunneling in supercooled water at temperatures close to its T_g. In addition, recent studies of LDA and ASW samples also revealed large isotope effect in T_g of water [90], being again consistent with the proposed here idea about tunneling in water at temperatures close to its T_g.

VI. Concluding Remarks

Our studies revealed unusually slow temperature variations of structural relaxation in vapor deposited water around its glass transition temperature T_g ~136K. It corresponds to the fragility index m ~14, by far the lowest known for any liquid. We ascribe this unusual behavior to quantum effects that are not negligible in water at these temperatures. The latter is confirmed by the analysis of neutron scattering data that revealed dominating contribution of quantum fluctuations to the mean squared atomic displacements at T~136K. Moreover, we speculate that these quantum effects maybe at the origin of the apparent dynamic crossover known for water (Fig.8).

The existence of significant quantum effects in water has its origin in the very light molecule and rather strong intermolecular interactions. Moreover, rotation of water molecule involves essentially only motion of the hydrogen atoms. Water is actually the lightest molecule that exists in a liquid state at ambient conditions. There are several other light molecules (e.g. NH_3, CH_4) that might also exhibit quantum effects at their respective glass transitions. It would be critically important to analyze these types of liquids to unravel how general this phenomenon may be for

other liquids. Also, detailed theoretical treatments of quantum effects in structural relaxation of liquids might be important for further understanding the behavior of water. These effects could remain measurable even at ambient conditions and affect proton transport and other phenomena in biological systems.

Acknowledgements

We thank C. A. Angell and P. Griffin for helpful discussions. This work was supported by UT-Battelle, LLC. AIK acknowledges the support by the DOE-BES, managed by UT-Battelle, LLC, for DOE under Contract DEAC05-00OR22725. UT team also thanks NSF for partial financial support under grant number CHE-1213444.

References

[1] O. Mishima and H. E. Stanley, Nature **396**, 329 (1998).

[2] C. A. Angell, Science **319**, 582 (2008).

[3] K. Ito, C. T. Moynihan, and C. A. Angell, Nature **398**, 492 (1999).

[4] R. S. Smith and B. D. Kay, Nature **398**, 788 (1999).

[5] P. G. Debenedetti, J. Phys.: Condens. Matter **15**, R1669 (2003).

[6] C. A. Angell, Annu. Rev. Phys. Chem. **55**, 559 (2004).

[7] V. Velikov, S. Borick, C.A. Angell, Science **294**, 2335 (2001).

[8] A. K. Soper, Nature Mater. **13**, 671 (2014).

[9] C. A. Angell, Nature Mater. **13**, 673 (2014).

[10] J. A. Sellberg, C. Huang, T. A. McQueen et al, Nature **510**, 381 (2014).

[11] M. Oguni, Y. Kanke, A. Nagoe, and S. Namba, J. Phys. Chem. B **115**, 14023 (2011).

[12] H. Jansson, R. Bergman, J. Swenson, J. Non-Cryst. Sol. **351** 2858 (2005).

[13] C.A. Angell, Chem. Rev. **102**, 2627 (2002).

[14] S. Cerveny, G. A. Schwartz, R. Bergman, and J. Swenson, Phys. Rev. Lett. **93**, 245702 (2004).

[15] G. P. Johari, J. Chem. Phys. **122**, 144508 (2005).

[16] J. Swenson, J. Phys.: Condens. Matter **16**, S5317 (2004).

[17] J.A. McMillan, S.C. Los, Nature **206**, 806 (1965).

[18] A. Hallbrucker, E. Mayer, G.P. Johari, J. Phys. Chem. **93**, 4986 (1989).

[19] G.P. Johari, A. Hallbrucker, E. Mayer, Nature **330**, 552 (1987).

[20] G.P. Johari, A. Hallbrucker, E. Mayer, Science **273**, 90 (1996).

[21] D.R. MacFarlane, C.A. Angell, J. Phys. Chem. **88**, 759 (1984).

[22] Y.P. Handa, D.D. Klug, J. Phys. Chem. **92**,3323 (1988).

[23] C.A. Tulk, D.D. Klug, R. Branderhorst, P. Sharpe, J.A. Ripmeester, J. Chem. Phys. **109**, 8478 (1998).

[24] M.S. Elsaesser, K. Winkel, E. Mayer, T. Loerting, Phys. Chem. Chem. Phys. **12**, 708 (2010).

[25] C. A. Angell, J. Phys. Chem. **97**, 6339 (1993).

[26] S.-H. Chen, L. Liu, E. Fratini, P. Baglioni, A. Faraone, and E. Mamontov, Proc. Natl. Acad. Sci. **103**, 9012 (2006).

[27] M. Vogel, Phys. Rev. Lett. **101**, 225701 (2008).

[28] F. Mallamace, M. Broccio, C. Corsaro, A. Faraone, U. Wanderlingh, L. Liu, C.-Y. Mou, and S. H. Chen, J. Chem. Phys. **124**, 161102 (2006).

[29] K.-I. Murata and H. Tanaka, Nat. Mater. **11**, 436 (2012).

[30] P. H. Poole, F. Sciortino, U. Essmann, and H. E. Stanley, Nature **360**, 324 (1992).

[31] P.H. Poole, I. Saika-Voivod, & F. Sciortino, J. Phys. Condens. Matter **17**, L431 (2005).

[32] M. Minozzi, P. Gallo, & M. Rovere, J. Mol. Liq. **127**, 28 (2006).

[33] J.L.F. Abascal, & C. Vega, J. Chem. Phys. **134**, 186101 (2011).

[34] Y. Liu, J.C. Palmer, A.Z. Panagiotopoulos, & P.G. Debenedetti, J. Chem. Phys. **137**, 214505 (2012).

[35] D. A. Fuentevilla and M. A. Anisimov, Phys. Rev. Lett. **97**, 195702 (2006)

[36] S. Sastry, P. G. Debenedetti, F. Sciortino, and H. E. Stanley, Phys. Rev. E **53**, 6144 (1996)

[37] J.C. Palmer, F. Martelli, Y. Liu, R. Car, A. Z. Panagiotopoulos & P. G. Debenedetti, Nature **510**, 385 (2014).

[38] O.J. Mishima, Chem. Phys. **133**, 144503 (2010).

[39] A. Faraone, L. Liu, C.-Y. Mou, C.-W. Yen, and S.-H. Chen, J. Chem. Phys. **121**, 10843 (2004).

[40] L. Liu, S.-H. Chen, A. Faraone, C.-W. Yen, and C.-Y. Mou, Phys. Rev. Lett. **95**, 117802 (2005).

[41] F. Mallamace, M. Broccio, C. Corsaro, A. Faraone, U. Wanderlingh, L.Liu, C. Y. Mou, and S. H. Chen, J. Chem. Phys. **124**, 161102 (2006).

[42] Y. Hayashi, A. Puzenko, I. Balin, Y.E. Ryabov and Y. Feldman, J. Phys. Chem. B **109**, 9174 (2005).

[43] D.T. Limmer, & D. Chandler, J. Chem. Phys.**135**, 134503 (2011).

[44] R. Bohmer, K. L. Ngai, C. A. Angell, and D. J. Plazek, J. Chem. Phys. **99**, 4201 (1993).

[45] D. Huang and G. B. McKenna, J. Chem. Phys. **114**, 5621 (2001).

[46] V. N. Novikov and A. P. Sokolov, Phys. Rev. Lett. **110**, 065701 (2013).

[47] S. Habershon, T. E. Markland, and D. E. Manolopoulos, J. Chem. Phys. **131**, 024501 (2009).

[48] T. F. Miller and D. E. Manolopoulos, J. Chem. Phys. **123**, 154504 (2005).

[49] J. A. Morrone and R. Car, Phys. Rev. Lett. **101**, 017801 (2008).

[50] A. Pietropaolo, R. Senesi, C. Andreani, A. Botti, M. A. Ricci, and F. Bruni, Phys. Rev. Lett. **100**, 127802 (2008).

[51] D. S. Olander and S. A. Rice, Proc. Natl. Acad. Sci. **69**, 98 (1972).

[52] S. La Spisa, M. Waldheim, J. Lintemoot, T. Thomas, J. Naff, and M. Robinson, J. Geophys. Res. Planets **106**, 33351 (2001).

[53] L. Yang, A. Guiseppi-Wilson, and P. Guiseppi-Elie, Biomed. Microdevices **13**, 279 (2011).

[54] M. Nakanishi, P. J. Griffin, E. Mamontov, and A. P. Sokolov, J. Chem. Phys. **136**, 124512 (2012).

[55] C. Gainaru, S. Kastner, F. Mayr, P. Lunkenheimer, S. Schildmann, H. J. Weber, W. Hiller, A. Loidl, and R. Böhmer, Phys. Rev. Lett. **107**, 118304 (2011).

[56] U. Kaatze, R. Behrends, and R. Pottel, J. Non-Cryst. Solids **305**, 19 (2002).

[57] W. Huang and R. Richert, J. Phys. Chem. B **112**, 9909 (2008).

[58] P. Jenniskens, D. F. Blake, and A. Kouchi, in Solar System Ices, edited by B. Schmitt, C. Bergh, and M. Festou (Springer Netherlands, 1998), pp. 139.

[59] A. I. Kolesnikov, J. C. Li, S. Dong, I. F. Bailey, R. S. Eccleston, W. Hahn, and S. F. Parker, Phys. Rev. Lett. **79**, 1869 (1997).

[60] J. Li and A. I. Kolesnikov, J. Mol. Liq. **100**, 1 (2002).

[61] J. Li, J. Chem. Phys. **105**, 6733 (1996).

[62] J. Penfold and J. Tomkinson, The ISIS time focused crystal analyser spectrometer TFXA. Report No. RAL-86-019, 20 p. (CCLRC ISIS TFXA, 1986).

[63] A. I. Kolesnikov and J. C. Li, Physica B: Cond. Mat. **234–236**, 34 (1997).

[64] P. Jenniskens and D. F. Blake, Astrophys. J. **473**, 1104 (1996).

[65] A. Ove, J. Phys.: Condens. Matter **20**, 244115 (2008).

[66] G. P. Johari, Phys. Chem. Chem. Phys. **7**, 1091 (2005).

[67] G. P. Johari, A. Hallbrucker, and E. Mayer, Nature **330**, 552 (1987).

[68] O. Yamamuro, M. Oguni, T. Matsuo, and H. Suga, J. Phys. Chem. Solids **48**, 935 (1987).

[69] S. R. Gough and D. W. Davidson, J. Chem. Phys. **52**, 5442 (1970).

[70] H. Suga and S. Seki, Faraday Discuss. Chem. Soc. **69**, 221 (1980).

[71] K. Amann-Winkel, C. Gainaru, P. H. Handle, M. Seidl, H. Nelson, R. Böhmer, and T. Loerting, Proc. Natl. Acad. Sci. **110**, 17720 (2013).

[72] L. Larini, A. Ottochian, C. De Michele, and D. Leporini, Nat. Phys. **4**, 42 (2008).

[73] R. W. Hall and P. G. Wolynes, J. Chem. Phys. **86**, 2943 (1987).

[74] U. Buchenau and R. Zorn, Europhys. Lett. **18**, 523 (1992).

[75] J. C. Dyre, N. B. Olsen, and T. Christensen, Phys. Rev. B **53**, 2171 (1996).

[76] P. Jenniskens and D. F. Blake, Science **265**, 753 (1994).

[77] M. C. Bellissent-Funel, L. Bosio, A. Hallbrucker, E. Mayer, and R. Sridi-Dorbez, J. Chem. Phys. **97**, 1282 (1992).

[78] D. D. Klug, E. Whalley, E. C. Svensson, J. H. Root, and V. F. Sears, Phys. Rev. B **44**, 841 (1991).

[79] A. Angell, Nat. Mater. **11**, 362 (2012).

[80] R. Buchner, J. Barthel, and J. Stauber, Chem. Phys. Lett. **306**, 57 (1999).

[81] P. Lunkenheimer, U. Schneider, R. Brand, and A. Loid, Contemp. Phys. **41**, 15 (2000).

[82] J. Qvist, H. Schober, and B. Halle, J.Chem. Phys. **134**, 144508 (2011)

[83] J. Qvist, C. Mattea, E.P Sunde & B. Halle, J.Chem.Phys.**136**, 204505 (2012).

[84] G. P. Johari and E. Whalley, J. Chem. Phys. **115**, 3274 (2001).

[85] O. Wörz and R. H. Cole J. Chem Phys. **51**, 1546 (1969).

[86] S.R. Gough and D.W. Davidson, J. Chem. Phys. **52**, 5442 (1970).

[87] F. Bruni, G. Consolini, and G. Careri, J. Chem. Phys. **99**, 538 (1993).

[88] M.-S. Chen, L. Onsager, J. Bonner, and J. Nagle, J. Chem. Phys. **60**, 405 (1974).

[89] S.F. Fisher and G.L. Hofacker, in *Physics of Ice*, ed. by N. Riehl, B. Bullemer, and H. Engelhardt (Plenum , New York, 1969), p.369.

[90] C. Gainaru, A. L. Agapov, V. Fuentes-Landete, et al, Pros. Nat. Ac. Sci., **111**, 17402 (2014).

Figure captions

FIG. 1**.** (Color online) a) Dielectric loss spectra of amorphous water measured on initial cooling and subsequent heating cycles. Amorphous water is stable at temperature below 150K. b) Crystallization of deposited water film occurs at temperatures above 150K with main relaxation peak irreversibly decreasing in amplitude and broadening in width. The order of temperatures corresponds to the order of lines.

FIG. 2. (Color online) Dielectric spectra of amorphous water (symbols) measured on initial cooling cycle in terms of a) storage and b) loss permittivity. Solid lines present the simultaneous fit of the real and imaginary spectra by the sum of three Cole-Cole functions.

FIG. 3**.** (Color online) Time-temperature superposition plot of the dielectric loss. Here, solid lines represent contributions of the individual processes: black (upper curve) – α-relaxation, blue (middle curve) – β-relaxation, green (bottom curve) – γ-relaxation processes.

FIG. 4. (Color online) Dynamical structure factor $S(Q,E)$ for LDA sample obtained from the INS spectra measured at T=15K: The experimental spectrum (red curve with squares), calculated multiphonon (black line) and single-phonon (blue curve with circles) contributions.

FIG. 5. (Color online) (a) Temperature dependence of characteristic relaxation times of different processes observed in the spectra of amorphous vapor-deposited water. In addition, empty stars are the data for cubic ice (from refs. [68, 69]) and empty pentagons present relaxation data of hexagonal ice (from ref. [70] and refs. therein). (b) Temperature dependence of τ_α vs inverse temperature (symbols) and its fit by the Arrhenius behavior (line). The latter provides estimates of the activation energy $E_a \approx 36\pm1$ kJ/mol and $\log_{10}[\tau_0\,(s)] = -10.9\pm0.3$.

FIG. 6. (Color online) MSD in LDA water and in vapor-deposited at low temperatures water (solid lines). The dashed line marks the expected $T_g \sim 136$K of water. Zero-point vibrations dominate MSD and contribute 55% -61% to the total MSD of amorphous water at T_g. The inset shows the generalized vibrational density of states $g(E)$ for inter-molecular vibrations in LDA and deposited water obtained from INS spectra [59-61].

FIG. 7. (Color online) Temperature dependence of the isothermal dielectric relaxation time (symbols) in the vapor-deposited film of water measured on cooling (open symbols) and on heating (closed symbols) vs T_g/T. T_g=135.6K was chosen as the temperature at which τ_α=1000 s. The slope of the temperature dependence indicates an unusually low value of fragility, m=14. The lines show the expected temperature dependence of $\tau_\alpha(T)$ estimated using Eq.(6) with the total MSD of deposited un-annealed sample (dashed line), with the total MSD of LDA water (solid line) and MSD with excluded zero-point vibrations for LDA water (dotted line). The total MSD of LDA reproduces the temperature dependence of $\tau_\alpha(T)$ well and emphasizes the importance of quantum fluctuations in the dynamics of deeply supercooled water.

FIG. 8. (Color online) Comparison of low- and high temperature data for the structural relaxation time in water and in glycerol. Open squares – dielectric spectroscopy data in water [80], solid circles – shifted viscosity data [25], stars – dielectric spectroscopy data in glycerol [81]. The dashed line presents approximation of the low temperature behavior by an Arrhenius dependence, the solid line is approximation of the high temperature behavior using the Vogel-Fulcher-Tammann function.

FIG. 9. (Color online) Schematic presentation of the potential well used to estimate tunneling probability. Lines in the well correspond to different quantum levels.